Available online at www.sciencedirect.com
SCIENCE DIRECT
Journal of Molecular Catalysis A: Chemical 244 (2006) 217–228
JOURNAL OF MOLECULAR CATALYSIS A: CHEMICAL
www.elsevier.com/locate/molcata

Morphology and control of Pd nanoparticles

Hwaipeng Choo [b,1], Baolin He [a], Kong Yong Liew [a,*], Hanfan Liu [a], Jinlin Li [a]

[a] *Hubei Key Laboratory for Catalysis and Material Science, South Central University for Nationalities, Wuhan 430074, China*
[b] *Department of Chemistry, Universiti Tunku Abdul Rahman, Kuala Lumpur, Malaysia*

Received 1 August 2005; received in revised form 3 August 2005; accepted 12 September 2005
Available online 17 October 2005

Abstract

Polymer-stabilized Pd nanoparticles synthesized by reduction of Pd salt with methanol are of various geometric shapes besides spherical. The TEM micrographs show that most of the triangular particles are plate-like although some tetrahedral particles are also observed. The four-sided rhombohedral and square particles and some of the hexagonal particles are plate-like as well. The pentagonal particles are decahedra formed from multiple twinning with imperfection. Most of the hexagonal particles and the icosahedral particles are imperfectly twinned. Extensive multiple twinning are observed under other synthesis conditions. Growing crystals were captured at intermediate stage of the particle formation. The proportion of the different morphologies could be varied by changing the conditions of the synthesis including the molar ratio of precursor salt: polymer, reducing agent, stabilizing polymer, reducing temperature and time, pH of the solution as well as average molecular weight of the polymer. A mechanism is proposed for the particle growth.

Keywords: Pd; Nanoparticles; Morphology; Control

1. Introduction

The catalytic activity and selectivity of metallic nanoparticles are strongly dependent on the particle size. It is also expected that the shape of the particles would affect the catalytic activity due to the changes of the surface-to-volume ratio and in the number of edges, corners and faces, as the morphology is varied [1]. Most nearly, monodispersed nanoparticles with sizes ranging from 1 to 20 nm assume near-spherical shape [2–4] as lower surface energy is associated with such geometry, although different morphologies have been detected.

Among the noble metal nanoparticles, the morphology of Pt has been most extensively studied. Mix structures of cubic, tetrahedral, irregular prismatic, icosahedral, octahedral [5,6], triangular, hexagonal as well as concave cubic [7], and nanowires Pt nanoparticles have been prepared. Spherical, rod-like and dendritic Ag nanoparticles as well as cubic Au and Ag nanoparticles have been prepared by pulse sonoelectrochemical method [8,9]. It is possible to prepare Cu particles with spherical to rod shapes [10]. For other protected noble metal colloidal nanoparticles without support, only sponge-like Ru [11], wire- and sponge-like Pd [12,13] decahedral, icosahedral, cuboctahedral, needle-like, flat-hexagonal and wire-like Ag [9,14,15] as well as decahedral, flat-triangular, rod- and plate-like Au particles [15–17] have been described.

Turkevich et al. discovered that colloidal Au particles were in plate forms rather than spheres [18]. Later, they reported that both the Pt and Pd particles can have plate-like structure with holes in the center and sharp edges [19]. However, the synthesis conditions for the regular plates were not reported. Sodium polyacrylate-stabilized Pd particles with large average diameter of 45 nm, prepared by reduction of palladium chloride solution with sodium formate, has been published but without description of their morphology and structures [20]. In addition, mixed structures of cuboctahedral, icosahedral, truncated decahedral or single twinned Pd particles have been reported [21–23]. We have previously reported [24] a preliminary study on the possibility of controlling the morphology of Pd nanoparticles in

* Corresponding author.
E-mail address: kongyongliew@yahoo.com.cn (K.Y. Liew).
[1] Present address: Motorola Technology Sdn. Bhd., Bayan Lepas Technoplex Industrial Park, 11900 Penang, Malaysia.

1381-1169/$ – see front matter © 2005 Elsevier B.V. All rights reserved.
doi:10.1016/j.molcata.2005.09.009

colloidal solution. In this paper, we describe in more detail the different morphologies of Pd colloidal nanoparticles and their control, prepared via chemical reduction in an aqueous environment using the polymer, PVP, as the stabilizing matrix.

2. Experimental

2.1. Materials and method

Palladium chloride (59% $PdCl_2$, Merck, Germany), chloroplatinic acid hexahydrate (40% $H_2PtCl_4{\cdot}6H_2O$, Merck, Germany and Beijing Chemicals), polyvinylpyrrolidone (PVP, average molecular weight, M_w = 10,000, 40,000 and 360,000, Sigma, St. Louis), polyvinylchloride (PVC, higher molecular weight, Sigma, St. Louis), polymethacylic acid sodium salt (PMAANa, 30 wt.% in H_2O, M_w = 6500, Aldrich, USA), sodium borohydride (Sigma, St. Louis) and sodium hydroxide (BDH, UK) were used as purchased. Methanol, ethanol, *n*-propanol, *i*-propanol, *N*,*N*-dimethylformamide (DMF) and hydrochloric acid (37%) (R&M, UK), aqueous ammonia (25 wt.%), were analytical grade reagents and used without further purification.

All the glass wares and magnetic bars were soaked with aqua-regia for a few days, then rinsed several times with distilled water and dried in an oven before used. The polymer-stabilized noble metal colloids were prepared according to a previously reported method [24]. An appropriate amount of the metal salt was dissolved in HCl solution, then, evaporated to dryness. The residue was again dissolved in an aqueous methanolic solution containing the stabilizing polymer to make up the required polymer:metal ratio. The resulting solution was refluxed or heated to an appropriate temperature to effect the reduction with or without addition of a 0.1 M methanolic NaOH.

2.2. Transmission electron microscopy (TEM)

The electron microscopy sample was prepared by placing a drop of the colloidal dispersion onto a copper grid followed by evaporating the solvent under ambient condition. The particle size and morphology were determined by TEM (Philips CM12 at 80–100 kV), while the crystalline structure of the metal nanoparticles was characterized with high-resolution TEM (HRTEM) (JEOL-2010 at 200 kV). Typically, the TEM micrographs of each sample were taken at multiple, random locations in the sample to ensure that the images reported are representative and at several magnifications, in order to obtain information about the sample in general as well as at closer visualization at higher magnifications and that the sample is not perturbed by the TEM beam. The average particle diameters were obtained by measuring >300 particles from the enlarged micrographs of each sample by using Image Analyst software (SIS Soft-Imaging Software, GmbH, Germany).

2.3. X-ray photoelectron spectroscopy (XPS)

XPS was recorded on an ESCALAB 2201-XL (VG Inc., Institute of Chemistry, Beijing) photoelectron spectrometer by using monochromatic Mg Kα radiation under vacuum at 2×10^{-6} Pa. The samples were dried under vacuum at room temperature prior to XPS measurement.

3. Results and discussion

Colloidal Pd nanoparticles were prepared by reduction of molar ratio of $PVP_{40\,K}$:Pd = 60:4 in aqueous methanolic solution at the refluxing temperature. XPS measurement showed only Pd $3d_{5/2}$ and $3d_{3/2}$ peaks at 339.6 and 334.4 eV, respectively, with reference to the C1s peak appearing at 284.6 eV, indicating that the Pd particles were in zero valence state. From the XRD diffraction pattern, the characteristic peaks for Pd at $2\theta = 40^\circ$, 47°, 68°, 82° and 86° corresponding to the (1 1 1), (2 0 0), (2 2 0), (3 1 1) and (2 2 2) lattice planes, respectively, were observed. The d-spacing and lattice constant were ∼0.223–0.225 and 0.386–0.390 nm, respectively, indicating the resultant particles were of pure Pd with FCC structure, in excellent agreement with those previously reported [2].

3.1. Structures of the geometric particles

A typical TEM micrograph of the Pd nanoparticles at lower magnification is shown in Fig. 1(a), while the dark field image is shown in Fig. 1(b). As can be seen, the particles are well-dispersed. The mean size and relative standard deviation are 12.6 and 0.34 nm, respectively. These images show that most of the particles have definite geometric shapes and are mostly single crystalline (SCP) with morphologies identifiable as spherical, triangular, rhombohedral or square, pentagonal and hexagonal-faced particles, while the remainders are twinned particles. Their distributions are: triangular, 47%; pentagonal, 24%; hexagonal, 22%; spherical, 3%; square or rhombohedral, 2%.

The small spherical particles are flat and generally shapeless (Fig. 2(a-i and a-ii)). These apparently flat particles have no internal features as the atomic fringes are displayed across the entire plane of the particles. These flat particles may be the precursor [6] for the larger particles, the morphologies of which are described below.

3.1.1. Triangular and hexagonal particles

Triangular particles of alumina-supported Pt catalyst showed plate-like morphology after a sintering process [25]. Further, trigonal lamellar particles of both the Au and Ag hydrosols [26] and hexagonal platelet of PVP protected Cu particles [27] have also been reported. We have found that, in the Pd colloid prepared, not just the triangular, but some of the hexagonal-faced particles existed in plate-like forms with sharp edges. Fig. 2(b-i) shows the plate-like triangular-faced particles, while Fig. 2(b-ii) shows the plate-like hexagonal-faced particle consisting of six atomic layers. Their structures are also confirmed by WBDF imaging as shown in Fig. 1(b). Both the triangular (T) and hexagonal (H)-faced particles show one to two fringes at the outer part of the particles, while no fringe is observed at the center, which is consistent with those reported for flat Ag nanoparticles [15]. This indicates that such particles are not the tetrahedral and cubooctahedral [27] types but plate-like. Very often, these triangular-faced particles are truncated at corners, giving rise

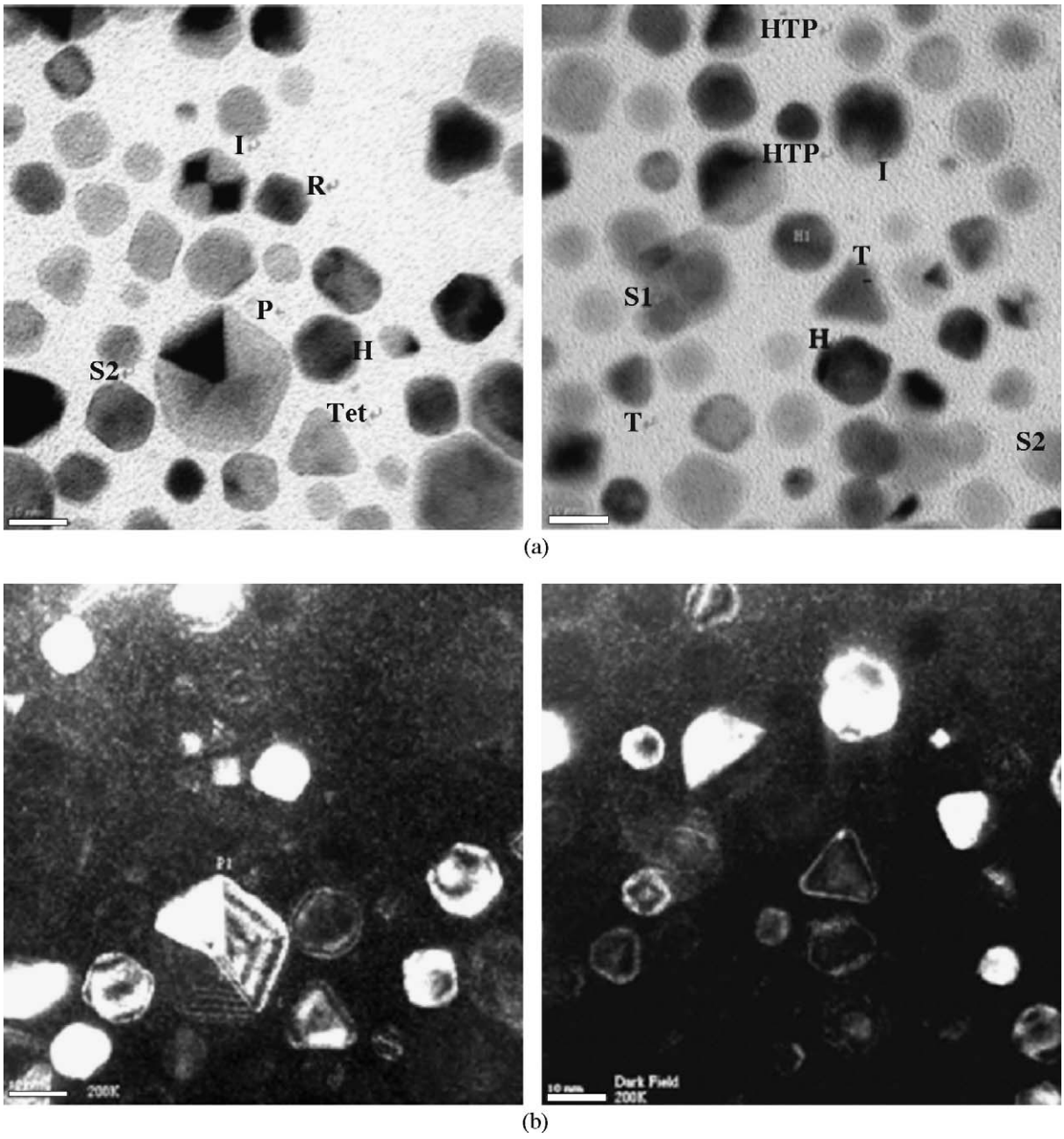

Fig. 1. TEM micrographs of Pd particles with molar ratio of PVP:Pd = 60:4 reduced with methanolic aqueous solution at refluxing temperature: (a) bright field and (b) dark field [scale bar 10 nm]; T: triangular; Tet: tetrahedral; Tt: truncated triangular; S: square pyramide; R: rhombohedral; P: pentagonal; H: hexagonal; HTP: twinned hexagonal.

to additional faces. However, one of the triangular shaped particles (marked Tet in Fig. 1(a)) shows three triangular faces in the dark field image, indicating the presence of tetrahedral particle.

3.1.2. Square and rhombohedral particles

There were two types of four-sided particles: square and rhombohedral. Normally, the square particles could have pyramidal or half-octahedral particles (0 0 1) base plane and four (1 1 1) side faces. As observed from the WBDF images (Fig. 1(b)), truncation parallel to the base plane may lead to the formation of two types of square particles, with additional (0 0 1) or (0 1 1) face. On higher magnification, it can be seen that the rhombohedral-faced particles were not the decahedral particles viewed in edge orientation [21]. Such particles have plate-like morphology (Fig. 2(c)) and frequently, have more rounded corners indicating the formation of additional higher index faces. Interestingly, an imperfection area on the first layer has been observed (white circle in Fig. 2(c-i)). This imperfection may accelerate the growth of the particle. Consequently, slight distortion resulted as can be seen on the left upper corner of the particle.

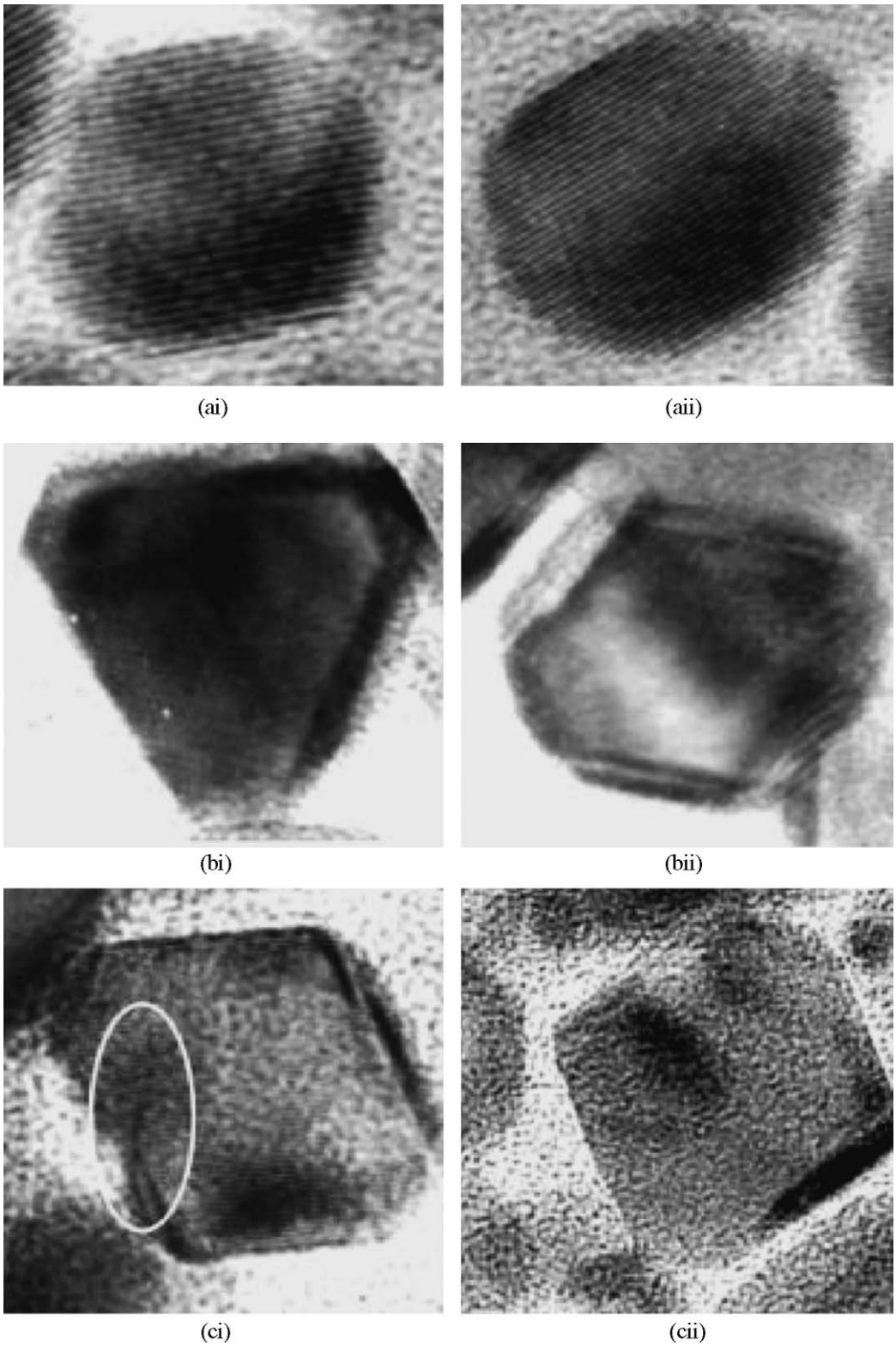

Fig. 2. (a) Small, apparently flat single crystals of Pd particles, believed to be the precursors of the larger flat particles [scale bar: 2 nm]. (b) Plate-like: (i) truncated triangular particle and (ii) hexagonal particle with six layers. (c) Plate-like rhombohedral-faced Pd particles with rounded corners and defect [scale bar: (i) 2 nm and (ii) 5 nm].

3.1.3. Pentagonal particles

The twinned particles in this study could be classified into two types of configuration: single twinned particles (STP), such as the hexagons and multiple twinned particles (MTP), such as the pentagonal decahedra and icosahedra. MTP occurred profusely in Ag and Au, but comparatively rarely in the other FCC or FCC-like materials [22]. It has been reported that particle morphologies with apparent five-fold symmetry were found only in the smaller particles, arising from strained polytetrahedral twinning, which cannot be maintained at larger particle sizes [9]. However, multiply twinned larger decahedra, are observed in the Pd colloid prepared in this study. It is well known that the MTP contained large non-homogeneous elastic strains [14]. Thus, dislocation must be introduced in order to release such strain [28]. Obviously, partial dislocations were found at the twin boundaries of decahedral particles (Fig. 3a). Such pseudo-crystalline particles observed in the WBDF image indicates that they have pentagonal bi-pyramid shape made up of five distorted FCC tetrahedra with almost the same size and a common five-fold axis (Fig. 1(b)). Very often, this kind of particles have more rounded edges and zigzagging twin boundaries with notches at the twin boundaries (black arrows in Fig. 3(b and c)). It have been reported that if a pentagonal bi-pyramid was constructed from five regular tetrahedral, so that there were four coherent twin boundaries on the {1 1 1} planes, an angular gap of about 7°20′ remained at the fifth boundary [29,30]. However, there is no experimental evidence to indicate any misfit between adjoining units [31], which is distributed throughout the particles by a relaxation of the FCC structure of each unit. However, we noticed that each segment did not assemble to a complete space filling structure in some decahedral particles. Indeed, small angular gaps associated with the zigzagging of boundaries are observed. As shown in Fig. 3(c), segments (D and E) are interconnected, while the first few atomic layers of segments (A–C) are disconnected near the vertex located at the center of the five-fold axis, the atomic lattice is not continuous. Another decahedral particle showing similar behavior is shown in Fig. 3(b) (white arrows). Duff et al. argued that

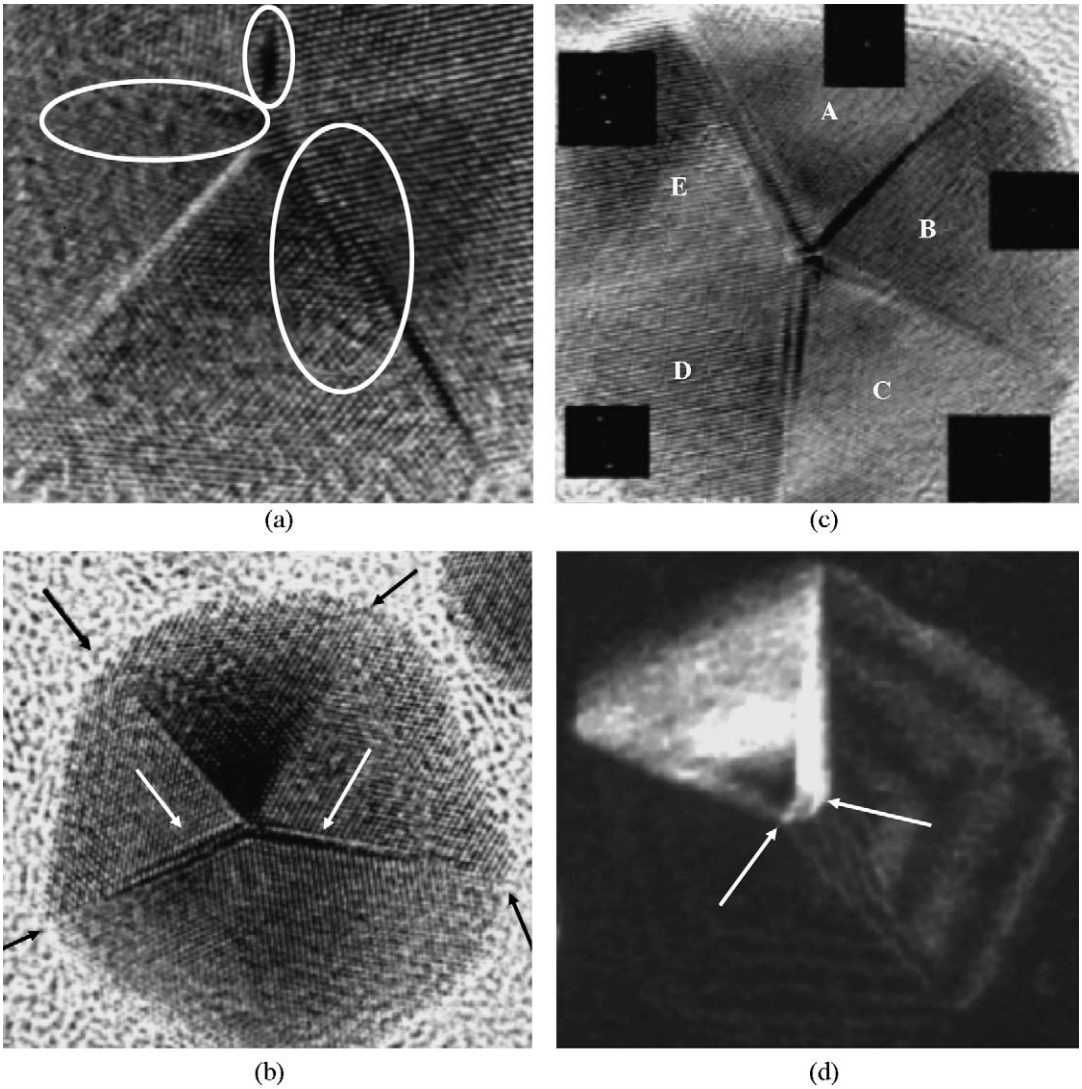

Fig. 3. HRTEM of decahedral Pd particles, which are made up of five distorted FCC tetrahedral: (a–c) partial dislocation and notches were found at zigzagging twin boundaries; (d) enlarged WBDF of the decahedral particles [scale bar (a–c): 2 nm].

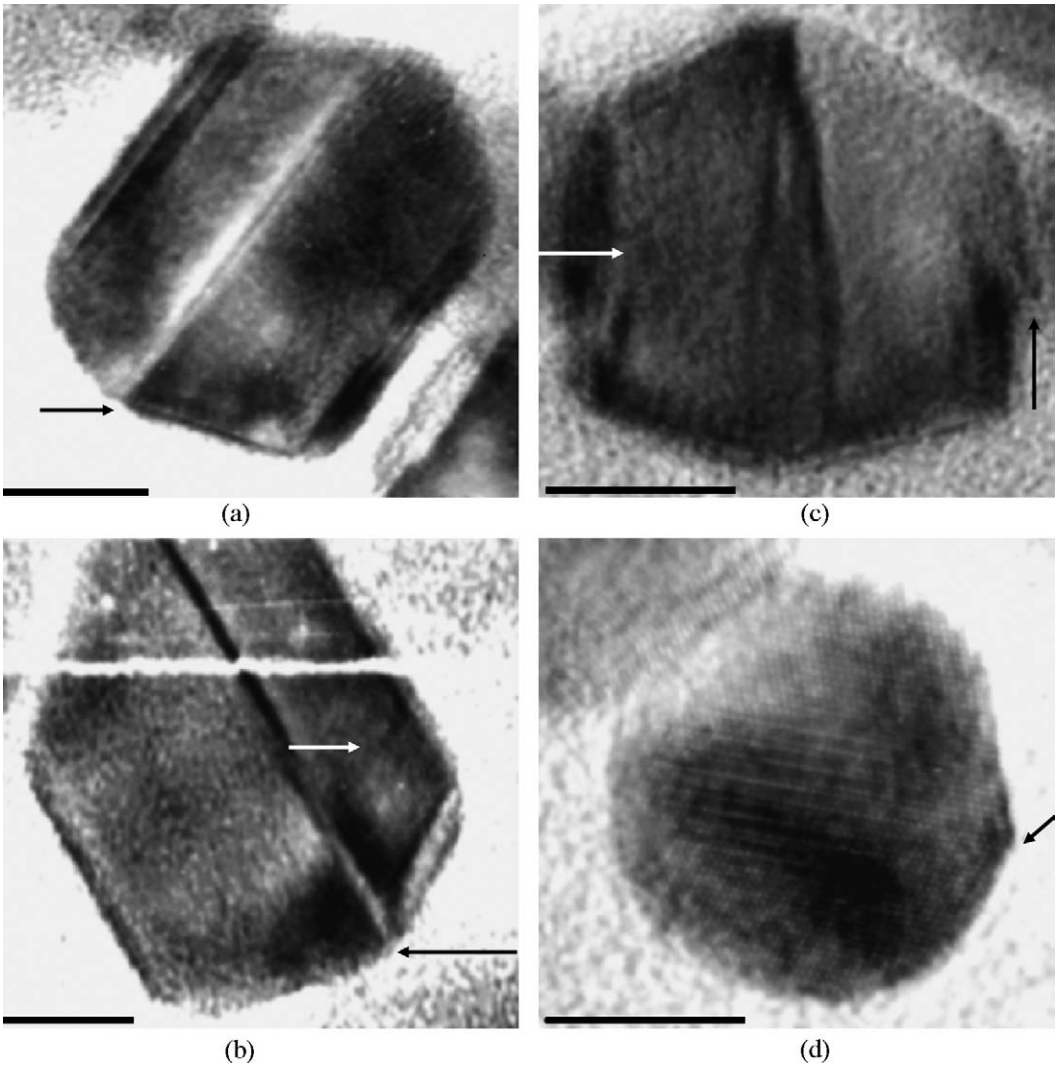

Fig. 4. Hexagonal twinned Pd particles (HTPs), which are made up of two trapezoid faces with one twin boundary: (a) regular particle; (b) a gap was found at the first few; atomic layers (black arrow); (c) HTP with wider groove, associated with incomplete growth; (d) HTP without obvious outline and twinned boundary [scale bar: 5 nm].

the metal–metal bond length parallel to the edges must expand under a homogeneous strain [32]. Our observation suggests that the strain could be removed by the disconnection of the first few atomic layers among the adjacent segments. Somehow, these atomic layers come close to each other when approaching the notches. The zigzagging boundaries behave similarly, the grooves become smaller near the notches. As shown in Fig. 3(d), the first atomic layer is not joined with its adjacent plane of other sub-units, whereas the second atomic layer does (white arrow). Such notches could be considered to act as preferential crystal growth sites as well as to minimize the surface energy of the particle [33].

3.2. Hexagonal twinned particles

Some of the hexagonal-faced particles composed of two trapezoid faces with one or two twin boundaries. These are referred to as the hexagonal twinned particles (HTP) and have previously been reported on supported Pt [25]. Similar to the decahedral particles, the HTP shows the zigzagging boundaries and notches (arrows in Fig. 4). Such particles do not have plate-like structure. The layer's sizes increased from the upper to the bottom. The HTP in Fig. 4(c) shows almost the same appearance except that a gap is found on the first few atomic layers at the twin boundary (black arrow), similar to the decahedral particle, the gap became narrower toward the opposite end. This may be attributed to the dislocation of the surface layers as indicated in Fig. 4(b) and may act as the preferential nucleation site for crystal growth, especially for the formation of multilayers HTP. An incomplete growth in HTP with notches and wider groove is observed as marked by arrows in Fig. 4(c). Fig. 4(d) shows one of the HTP without obvious outline and twinned boundary.

3.2.1. Icosahedral particles

Icosahedral particles composed of 20 FCC tetrahedras are rarely seen in samples with larger particle size. A large icosahedral particle with two-fold symmetry axis and a "butterfly-like" contrast is shown in Fig. 1. The particle as shown in Fig. 5(a)

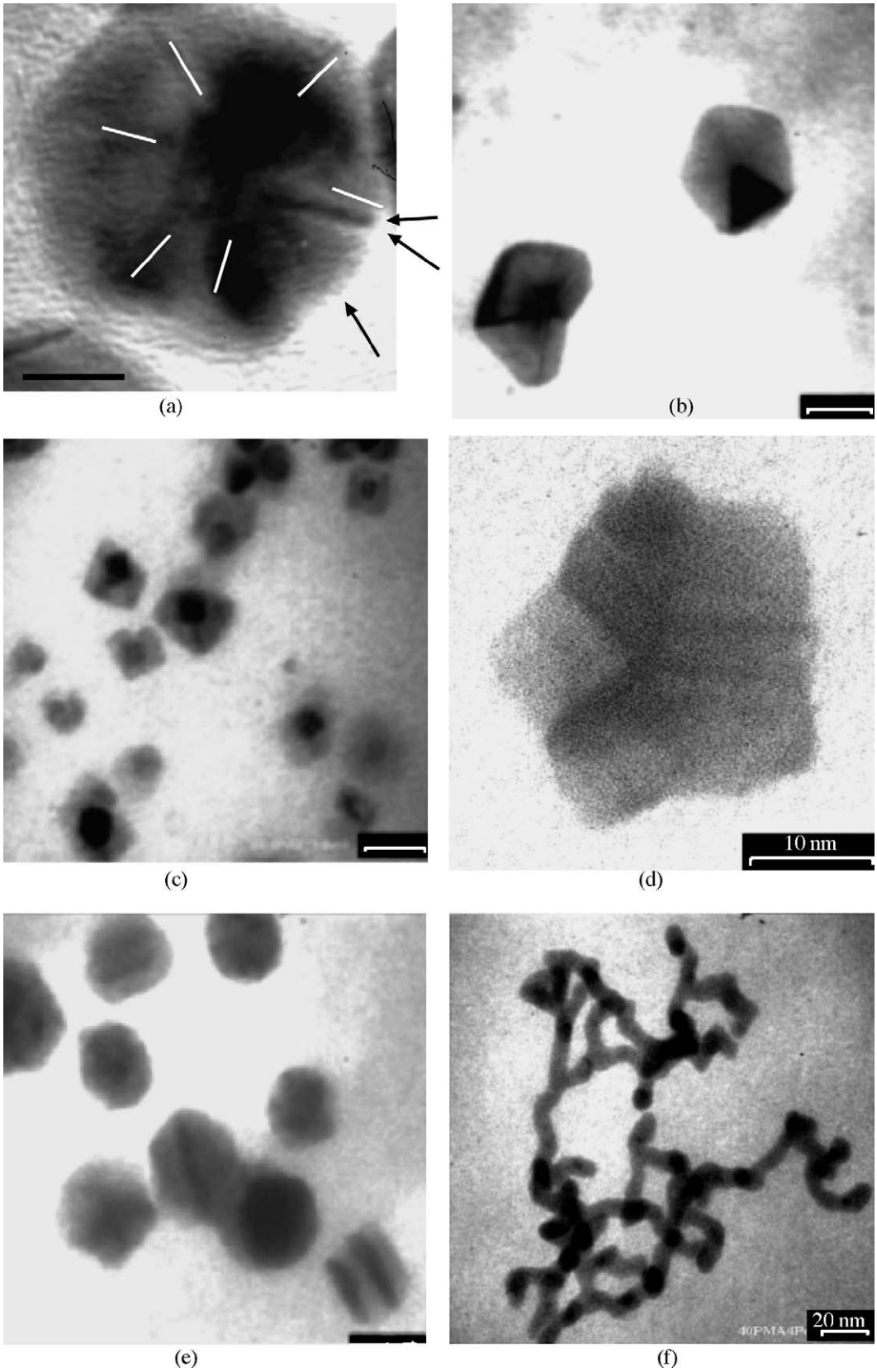

Fig. 5. (a) Icosahedral Pd nanoparticles with residual three-fold axis, but with eight individual components [scale bar: 5 nm]. (b) Pd nanoparticles stabilized with PVP_{10K} molar ratio PVP:Pd = 60:4 reduced by methanol at 50 °C for 3 h. (c) Pd nanoparticles stabilized with PVP_{40K} molar ratio of PVP:Pd = 60:4 at 60 °C for 30 min. (d) PMMANa stabilized Pd nanoparticles with molar ratio of polymer:Pd = 60:4 reduced by DMF at refluxing temperature for 3 h. (e) PVC stabilized Pd nanoparticles with molar ratio of PVC:Pd = 60:4 reduced by DMF at refluxing temperature for 3 h (f) PMMANa stabilized with molar ratio of polymer:Pd = 40:4 reduced by methanol at reflux for 3 h.

has a three-fold symmetry axis, but it is also of the icosahedral type. The particle now contains two extra units, i.e. one of the original six units having apparently divided into three sub-units as indicated by the black arrows. At least one of the boundaries was no longer coincidental with a crystallographic direction. Similar observation on decahedral Ag colloidal particles has been reported and explained that as the particle size increased, a fundamental change in microstructure took place [34]. The structural mismatch imposed by the non-FCC nucleus became incompatible with the normal FCC packing, dislocations must be introduced on further growth.

3.3. Morphology distribution

3.3.1. Effect of Pd precursor concentration

No geometrical shape other than spherical or near-spherical was observed for the smaller nanoparticles with $PVP_{40\,K}$:Pd ratio of 40:1. When the concentration of Pd precursor was increased with constant $PVP_{40\,K}$ concentration, truncated triangular, four-sided, pentagonal and hexagonal particles are the most frequently observed face shapes. Additionally, some of these geometrical particles became twinned to form more complicated structures. Two of these multiply twinned particles formed at lower temperature when the rate of reduction was lowered are shown in Fig. 5(b).

The relative percentages of the various modifications of the particles in different colloids are shown in Fig. 6. Almost 20% of the particles in the colloid with $PVP_{40\,K}$:Pd = 40:2 have geometrical shapes with the majority being hexagonal, while more than 90% of the particles showed geometrical shapes at higher Pd precursor concentration. The predominant morphology in $PVP_{40\,K}$:Pd = 40:3 was hexagonal-faced particles. The proportion of this type of particles decreased, whereas the proportion of triangular-faced particles increased, reaching more than 30% when the $PVP_{40\,K}$:Pd ratio was increased to 40:4. This could be possible if deposition of the subsequently reduced atoms occurred preferentially on faces of the initially formed seeds leading to hexagonal morphology and then transformed to triangular-faced particles as they grew. Large amount of Pd precursor is, thus, needed for the formation of triangular face particles. Not much variation was observed for other face shape particles as the precursor concentration was changed.

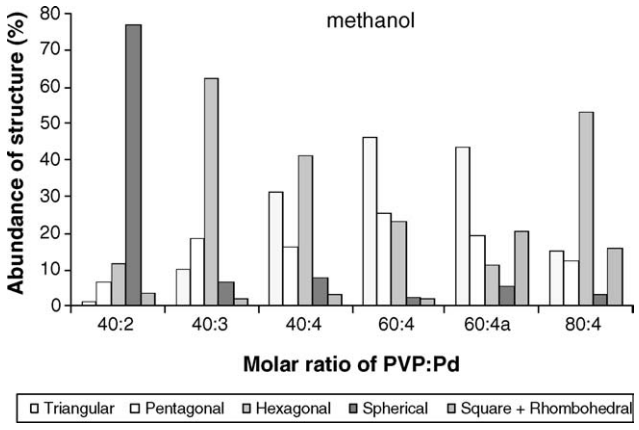

Fig. 6. Morphological distribution of $PVP_{40\,K}$:Pd with molar ratio of 40:2, 40:3, 40:4, 60:4, 60:4(a) (without 0.1 M NaOH) and 80:4, after refluxing in methanolic aqueous solution for 3 h.

3.3.2. Effect of PVP concentration

As shown in Fig. 6, by keeping the Pd precursor concentration constant but increasing the amount of $PVP_{40\,K}$ by 50% as in colloid with $PVP_{40\,K}$:Pd = 60:4, the proportion of the triangular face particles increased to more than 45% with a decrease in the four-sided and hexagonal face particles. However, the proportion of triangular face particles decreased markedly, while the proportion of hexagonal and four-sided face particles increased distinctly as the concentration of $PVP_{40\,K}$ was again increased by 50%. The large number of shadowed dark clusters as shown in Fig. 5(e) may, presumably, consist of reduced nuclei before crystal formation together with their associated polymers. Thus, in the presence of such large quantity of polymer as in the case of $PVP_{40\,K}$:Pd = 80:4, the PVP surrounding the particles or present in the solution may act as a barrier to prevent further growth of the hexagonal face particles hence smaller amount of triangular face particles resulted. The proportion of pentagonal face particles increased and reached a maximum value of ~26% at $PVP_{40\,K}$:Pd = 60:4, then decreased to ~12% at $PVP_{40\,K}$:Pd = 80:4 (Fig. 6). Particles with five-fold symmetry are energetically favored at the early stage of growth. Thus, the formation of such particles may be inhibited with the excess of $PVP_{40\,K}$ hence lower percentage of pentagonal face particles. However, the formation of four-sided particles was favored with high concentration of $PVP_{40\,K}$. The optimum condition for the formation of triangular and pentagonal face particles was found at $PVP_{40\,K}$:Pd = 60:4. Such $PVP_{40\,K}$ concentration was apparently not large enough to prohibit the shape transformation process or, to prevent the particles from growth. Thus, the formations of the triangular and pentagonal face particles are different to those of the hexagonal face particles.

3.3.3. Effect of pH of solution

Addition of base accelerates the reduction rate for Pd precursor [6]. We noticed that the presence of base can also affect the morphology of the Pd nanoparticles. Regular triangular face particles were favored rather than the truncated triangular particles in the absence of NaOH although both of the $PVP_{40\,K}$:Pd = 60:4 and 60:4(a) have almost the same triangular distribution (Fig. 6). The four-sided particles increased markedly, while the pentagonal and hexagonal face particles decreased in the absence of NaOH, perhaps, due to the slower nucleation rate relative to the growth rate.

Another additive base, i.e. 0.1 M methanolic NH_3, was also used to study its effect on the morphology changes. Particles with well-defined geometrical shapes have been produced in the presence of 5 ml of methanolic NaOH at pH ~ 2.5. However, no particle with geometrical shape other than spherical particles was found when the NaOH was replaced by 20 ml of methanolic NH_3 at pH ~ 2.2. It is noticed that some of these particles were surrounded by an outer grey layer: either completely or partially (Fig. 5(d)). Thus, a Pd core–Pd shell structure could be formed from this encapsulation process.

The pH of the solution plays an important role on the morphology control of the particles. It is observed that the formed particles with geometrical shapes disappeared when the pH of the solution increased from pH ∼ 2.5–10.2. The distinct outline of the shaped particles became rounded and finally spherical or near-spherical, due to the increase of the reduction rate associated with the increase of pH.

On the other hand, particles transformed from spherical or near-spherical shape to geometrical shapes when the amount of methanolic NH_3 was increased Triangular, hexagonal and four-sided shapes were the most frequently observed, while pentagonal particles were rarely found. The presence of a complexing agent may have resulted in a slower reduction rate, and thus, larger particles with geometrical shapes were generated.

3.3.4. Effect of average molecular weight of PVP

The effect of the variation of the average molecular weight of the stabilizing polymer, M_w, on particles size was not significantly. However, the influence was evident on the morphological distribution of Pd particles as shown in Fig. 7 in contrast to those observed by other workers [35,36], who claimed that the M_w of PVP did not have marked influence on the morphology of Au and Pt nanoparticles. However, the influence was not as evident as in the case of increasing the concentration of $PVP_{40\,K}$. In both methanolic and *i*-propanolic solutions, as the M_w of PVP was increased from 10,000 to 40,000, then to 360,000, the percentage of the hexagonal and four-sided face particles decreased then increased again, whereas the percentage of the triangular as well as pentagonal face particles increased then decreased. This may be attributed to the number of polymer molecules present in the system. The number of polymer molecules increased with a decrease of M_w when the same weight of PVP was used. $PVP_{10\,K}$ was presumably coordinated more strongly to the reduced particles. Thus, the formations of triangular and pentagonal face particles were hindered, while the hexagonal face particles were promoted in the presence of a larger number of polymer molecules. The particles continued to grow in the environment consisting of $PVP_{360\,K}$ and $PVP_{40\,K}$ as compared to those of $PVP_{10\,K}$, hence, higher percentage of triangular and pentagonal face particles were obtained. The optimum condition for the formation of triangular and pentagonal face particles was found at $PVP_{40\,K}$. Generally, four-sided face particles were the dominant particle shape in the presence of *i*-propanol. The stabilizing efficiency of $PVP_{10\,K}$ in methanolic solution with higher concentration of Pd precursor salt was poorer than those of $PVP_{40\,K}$ and $PVP_{360\,K}$ as two distinct sizes of particles were formed. Most of the larger particles were in hexagonal face shape, whereas most of the smaller particles existed in other face shapes, indicating that the hexagonal face particles were more easily formed.

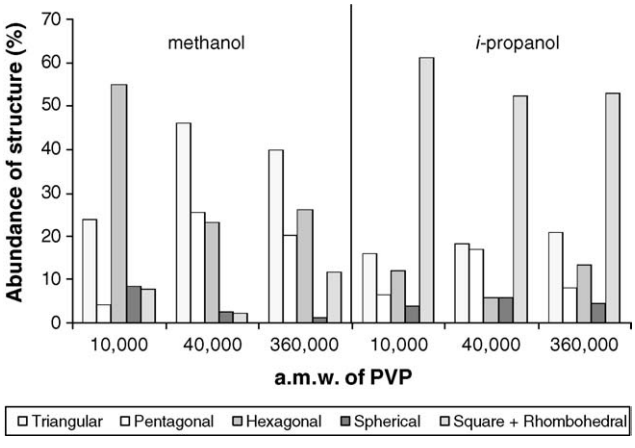

Fig. 7. Morphological distribution of Pd nanoparticles stabilized by PVP with different average molecular weights and molar ratio of 60:4, after refluxing in methanolic and *i*-propanolic aqueous solution for 3 h.

3.3.5. Effect of reducing agent

Reducing agents with different activities can give rise to different particle sizes [1,2]. We found that different reducing agents gave rise to different morphologies with higher precursor salt concentration. Spherical or near-spherical particles with smaller size were favored with strong reducing agent. Particles with geometrical shapes began to appear as the reducing ability of the agent decreased. More particles with non-distinct outline were formed in the presence of 2-methoxyethanol and 2-butoxyethanol and hexagonal particles were the predominant shape in ethylene glycol.

Interestingly, sponge-like structure rather than an agglomeration of small Pd crystallites were found with DMF. However, some of the Pd particles with smaller size existed in near-spherical shape. It has been reported that the reducing activity of DMF was higher than ethanol [37]. Thus, the formation of the sponge-like structure may be due to the rapid nucleation with much faster formation rate as reported for the sponge-like Au and Pd particles reduced by $LiBEt_3H$ in block copolymers micelles [22]. Although the effect of alcohols on particle size has been long studied, the effect of alcohols on morphology has not been reported. We found that using different alcohols as reducing agents at their respective refluxing temperature can affect the morphology of nanoparticles formed. Triangular face particles were the majority in methanol (∼46%), while hexagonal and four-sided face particles were dominant in aqueous *n*-propanol (∼69%) and *i*-propanol (∼51%) solutions, respectively (Fig. 8). It is observed that larger particles showed well-defined face shape, whereas the smaller ones are spherical or near-spherical with ethanol, *n*-butanol and *i*-butanol as reducing agents. This may be attributed to the higher reducing ability of ethanol as well as the stronger solubility of PVP molecules in aqueous ethanol than in alcohols with longer carbon chains. Both *n*-butanol and *i*-butanol are only moderately soluble in water, with *n*-butanol slightly lower than *i*-butanol.

Besides organic solvents, hydrogen gas as well as sodium borohydride salt were also used as reducing agents in this study. It is well known that both H_2 and $NaBH_4$ are strong reducing agents even at ambient temperature. The preparation of samples with molar ratio of $PVP_{40\,K}$:Pd = 60:4 was performed at room temperature for 3 h. It was observed that particles reduced by H_2 and $NaBH_4$ showed different morphologies as compared to those reduced by methanol. Larger spherical particles were formed with H_2 and irregularly shaped particles were produced with $NaBH_4$.

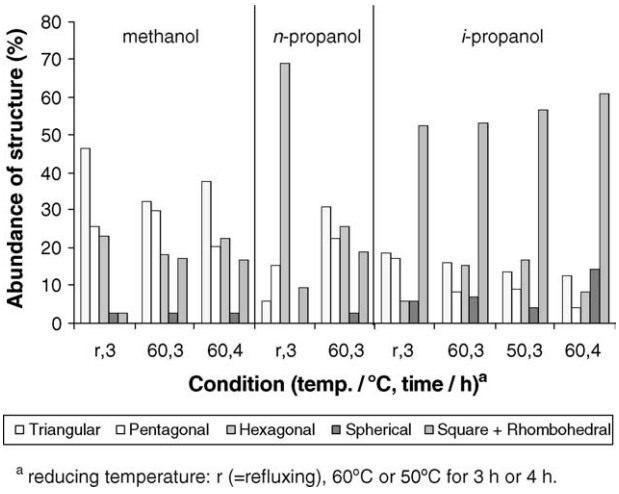

Fig. 8. Morphological distribution of $PVP_{40\,K}$–Pd nanoparticles with molar ratio of 60:4, after heating in methanolic, *n*-propanolic and *i*-propanolic aqueous solution for 3–4 h at temperatures: 50, 60 °C and refluxing temperature.

3.3.6. Effect of reduction temperature and time

Reduction with short-chain alcohols at various temperatures were carried out and the morphological distribution is shown in Fig. 8. Methanol, *n*-propanol and *i*-propanol were chosen as they produced regular shape particles with distinct outline. No colloidal dispersion was formed when the reaction was carried out at 40 °C for 3 h in aqueous methanolic solution. However, well-defined nanoparticles were formed when the temperature was maintained at 60 °C for 3 h. Regular, instead of truncated, triangular particles were formed and four-sided particles increased obviously (Fig. 8) at this temperature. These may be caused by the rather slow reduction rate at the lower temperature, which is consistent with the previous observation that regular triangular face particles were favored with slower reduction rate as in the absence of NaOH additive base. It is also noticed that some of the particles were not at their final stage of growth with the Pd cores enclosed by grey outer shades as described previously. Another experiment was carried out at longer reducing time, i.e. 60 °C for 4 h. The grey shades disappeared. As a result, concave particles with more rounded corners have been formed, more elongated particles were present in such environment. Thus, it seems possible to synthesis rod-like particles by lengthening the reaction time at lower reducing temperature.

From the TEM micrographs of Pd nanoparticles reduced by aqueous *n*-propanolic solutions at 50 °C and 60 °C, the morphological distribution changed as the reducing temperature increased; the hexagonal particles decreased markedly from ~70 to <25%, while the triangular, pentagonal and four-sided particles increased at 60 °C for 3 h (Fig. 8). No particular shape particles were dominant in such condition; triangular, pentagonal, hexagonal and four-sided particles are in similar proportion. Again, regular triangular particles were favored due to the slower reduction rate at lower reducing temperature.

Four-sided face particles were always the dominant shape (>50%) in *i*-propanolic solution at all the reaction conditions (Fig. 8). The proportion of the four-sided particles did not change much, the triangular and pentagonal face particles decreased slightly, whereas the hexagonal face particles increased as the reducing temperature was decreased. By lengthening the reducing time at lower temperature, i.e. 60 °C for 4 h, it is noticed that the percentage of the spherical or near-spherical shape particles in *i*-propanolic solution increased. Besides, it is observed that small amount of the four-sided particles were also surrounded by grey outer layers. This indicates that these four-sided face particles grew much slower but continuously, especially at lower temperature. However, this grey layer did not show differing contrasts and was distributed homogeneously, which was different from that previously described for reduction at 60 °C in methanolic solution. The face shape of the core was usually oriented 45° to the outer layer. Ridges from the center to the opposite angles can be seen clearly.

Besides, the Pd colloids stabilized by $PVP_{40\,K}$, another Pd colloid stabilized by $PVP_{10\,K}$ with similar molar ratio of $PVP_{10\,K}$:Pd = 60:4 have been prepared by refluxing in methanolic solution at 50 °C for 3 h and was used to study the thermal effect on the morphologies of particles formed. It was found that large and small particles coexisted. The small particles were spherical or near-spherical, while the larger ones showed well-defined morphologies with triangular, pentagonal, hexagonal and four-sided face shapes. Unlike the $PVP_{10\,K}$–Pd colloid prepared at refluxing temperature, hexagonal face particles were no longer dominant. It is noticed that one of the units of the pentagonal particle has more rounded outline, instead of sharp outline, as indicated by the arrow in Fig. 5(a). Surprisingly, we also found that the growth of the pentagonal particles were incomplete in this synthesis condition. These incomplete pentagonal particles were composed of three sub-units, presumably from three triangular plate particles as the depth was equivalent along the length of the twin boundaries. Unlike the strained decahedral particles with the vertex protruding out of the plane, particles of this type are suspected to contain less strain and appear to be flat.

3.3.7. Effect of stabilizing polymer

In order to study the effect of stabilizing material on the morphologies of the Pd nanoparticles, PVC, instead of PVP, was used for the preparation of colloid with molar ratio of PVC:Pd = 60:4. Since PVC is not readily soluble in water and alcohols, DMF was chosen as the reducing agent as well as the solvent in this case. Unlike the Pd particles formed in PVP–DMF–H_2O environment, the PVC-stabilized Pd particles have larger mean size and well-defined outline, having similar features as those stabilized by PVP in alcoholic aqueous solutions. However, it is noticed that on higher magnification, most of the Pd particles were twinned rather than SCPs (Fig. 5(b)). Most of the PVC-stabilized Pd twinned particles have more than one twin boundaries with re-entrant surface features, as shown in Fig. 5(c). The twinned boundaries were parallel to each other with the exception of the pentagonal and some hexagonal face particles. Normally, the decahedral particles have five twinned boundaries. However, particle with five-fold axis residual and contained more than five individual units existed. Such particles have seven twinned boundaries and two of the boundaries were no longer in the crystallographic direction. Apparently, PVC has lower stabiliz-

ing efficiency than PVP as smaller number of the large particles was formed.

The newly formed particles in an environment with less protection were not stable enough. DMF has greater reducing activity; the fast reduction may lead to the formation of smaller particles or nuclei with non-FCC packing. Re-attachment of smaller particles seems to be an alternative pathway for forming stable particles. These smaller SCPs may undergo coalescence giving rise to a series of parallel twinned boundaries accompanied by re-entrant surface features. It is believed that the re-entrant surface has similar function as notch to reduce the total surface energy of the particles [38,39]. In addition, nucleation was suspected to occur preferentially on such re-entrant surface hence crystal growth in one direction was accelerated, explaining why most of the four-sided face particles here have rectangular face shape instead of square or rhombohedral face shape. Some of the particles showed various contrasts, indicating many crystalline defects. Most of the particles were not symmetrical, presumably, due to the fast-growing process.

Other than PVC, the stabilizing efficiency of PMAANa on Pd particles was also investigated. Colloid with molar ratio of PMAANa:Pd = 40:4 in methanolic aqueous solution was prepared at refluxing temperature for 3 h. The PMAANa-stabilized Pd particles showed novel peanut-like nanostructure, which is totally different features from those of $PVP_{40\,K}$-stabilized Pd particles. This may be attributed to the poorer stabilizing efficiency of PMAANa. Some of these peanut-like nanostructures interconnected among themselves and fused into nanowires (Fig. 5(f)), which have almost the same diameter as the peanut-like particles. It is inferred that this long-range nanonetwork, peanut-like nanostructure and well-separated nanoparticles may interchange via disintegration and collision by manipulating the reaction conditions. As far as we can ascertain, such peanut- and wire-like structures for Pd particles prepared via colloidal route have not been reported.

4. Conclusion

Several different growth mechanisms for the formation of metal nanoparticles have been proposed. By referring to other reported results [21–23,25,28] as well as the experimental results obtained in this study, a model for the formation of the geometric particles is proposed. The metal salt is first reduced to zero valence metal atoms. These atoms may collide in solution with further metal ions, metal atoms or clusters to form an irreversible "seed" of stable metal nuclei. These nuclei then grew into larger particles during the "ripening" (Ostward) process via migration–coalescence, interparticle transport and edge adsorption growth. As described by previous authors, particle migration and coalescence played a predominant role when the particles were small, while the fast-growing particles with some crystallographic characteristic facilitated growth by an interparticle transport mechanism. Besides, the particle growth also appeared to go through an edge or surface adsorption process.

Various shapes of particles coexisted in this study. The internal structure of these particles may have been formed at the early stage of the reduction, then proceed by growth. It has been reported that of the stable precursor nuclei leading to common morphologies, namely icosahedral, decahedral, cuboctahedral, octahedral and tetrahedral; only, the last can be modified simply to give trigonal and hexagonal platelets [26]. The initial precursor nucleus for the trigonal and hexagonal platelet particles must, therefore, contain unique three- and six-fold axes, which are expressed in the developed particles, respectively. They proposed that if a regular FCC tetrahedral is truncated on a (1 1 1) surface and then twinned by reflection at this surface, a suitable nucleus for the trigonal lamellar particles can be obtained. Alternatively, a reflection twin on (1 1 1) followed by a 30° rotation about the three-fold axis normal to the twin plane may lead to a precursor nucleus of a plate-like hexagon which no longer contains a twin plane since the twin is effectively eliminated by the rotation.

The generation of multiple parallel twins may arise either from further reflection twinning of tetrahedral at an early stage in the growth process or from the migration and dissociation of partial defects parallel to the upper and lower surfaces of the particle. Twinning is the favorable pathway for MTP when the particles were small due to insufficient activation energy. However, the origin of the twin boundaries remained unclear. One possibility is that twins arise as a consequence of particle coalescence. Insufficient protection from stabilizer, for instance in PVC environment, may be the reason that multiple twinning predominated. This is consistent with the prediction that if the surface of a metal can be compressed by some means, the decahedral and/or icosahedral particles of the metal will be produced in solution [40]. As a comparison to decahedral particles, icosahedral particles were found less in the larger particle size range. This may be attributed to the fact that icosahedron has a more compressed structure than that of decahedra [41]. Any defects, such as dislocation and twinning, can be attributed to the growth process, as the initial nanocrystals were defect-free [28].

It is noticed that the various shapes of Pd particle are in competition to each other. The occurrence and frequency of these kinds of particles at the end of the experiment may depend on several factors, such as molar ratio of metal salt and polymer, reducing agent, stabilizing polymer and additive base, reducing temperature and time, pH of the solution as well as average molecular weight of the polymer. Capping molecules are capable of differentiating between crystal planes and exhibit different adsorption affinities to these planes, resulting in particles with non-spherical shape [5]. The exposure of the various crystal planes to the polymer environment results in the adsorption of the polymer to the crystal plane and once adsorbed, the polymer prevents the growth of the particles in the direction perpendicular to the interface and hence, the growth of the particles proceeds in other directions. Thus, it is deduced that effective growth sites on small particles/nuclei are not homogeneously distributed although nucleation is considerably homogeneous in well-stirred solution in all the colloids. The structural transformations may sometimes contribute towards a lowering of the internal energy of the particles, balancing the increase in surface energy caused by the addition and motion of atomic columns at the particle surfaces.

Acknowledgement

A research Grant No. 2003ABA027 from Hubei Natural Science Foundation is gratefully acknowledged.

References

[1] R. Narayan, M.A. El-Sayed, J. Am. Chem. Soc. 126 (2004) 7194–7195.
[2] H. Hirai, Y. Nakao, N. Toshima, J. Macromol. Sci. Chem. A13 (6) (1979) 727–750.
[3] T. Teranishi, M. Miyake, Chem. Mater. 10 (2) (1998) 594–600.
[4] X. Yan, H. Liu, K.Y. Liew, J. Mater. Chem. 11 (2001) 3387–3391.
[5] T.S. Ahmadi, Z.L. Wang, T.C. Green, A. Henglein, M.A. El-Sayed, Science 272 (1998) 1924–1926.
[6] X. Fu, Y. Wang, N. Wu, L. Gui, Y. Tang, Langmuir 18 (12) (2002) 4619–4624.
[7] K.V. Sarathy, G. Raina, R.T. Yadav, G.U. Kulkarni, C.N.R. Rao, J. Phys. Chem. B 101 (48) (1997) 9876–9880.
[8] Y. Sun, Y. Xia, Science 298 (2002) 2176.
[9] Y. Sun, Y. Xia, Adv. Mater. 14 (11) (2002) 833–837.
[10] J. Tanori, N. Duxin, C. Petit, I. Lisiecki, P. Veillet, M.P. Pileni, Colloid Polym. Sci. 273 (1995) 886–892.
[11] O. Vidoni, K. Philippot, C. Amiens, B. Chaudret, O. Balmes, J. Malm, J. Bovin, F. Senocq, M. Casanove, Angew. Chem. Int. Ed. Engl. 38 (24) (1999) 3736–3738.
[12] E.C. Walter, R.M. Penner, H. Liu, K.H. Ng, M.P. Zach, F. Favier, Surf. Interface Anal. 34 (2002) 409–412.
[13] M. Antonietti, C. Goltner, Angew. Chem. Int. Ed. Engl. 36 (1997) 910–928.
[14] L.D. Marks, A. Howie, Nature 282 (1979) 198.
[15] A. Henglein, M. Giersig, J. Phys. Chem. B 103 (44) (1999) 9533–9539.
[16] Y. Yu, S. Chang, C. Lee, C.R. Chris Wang, J. Phys. Chem. B 101 (34) (1997) 6661–6664.
[17] Y. Zhou, C.Y. Wang, Y.R. Zhu, Z.Y. Chen, Chem. Mater. 11 (9) (1999) 2310–2312.
[18] J. Turkevich, P.C. Stevenson, J. Hillier, Discuss. Faraday Soc. 11 (1951) 55–75.
[19] Y. Chiang, J. Turkevich, J. Colloid Sci. 18 (1983) 772–783.
[20] J. Turkevich, G. Kim, Science 169 (1970) 873–879.
[21] F. Robinson, M. Gillet, Thin Solid Films 98 (1982) 179–198.
[22] L.D. Marks, A. Howie, D.J. Smith, Conf. Ser. Inst. Phys. (Bristol) 52 (1980) 397–401.
[23] S. Giorgio, H. Graoui, C.R. Henry, C. Chapon, Mater. Sci. Eng. A229 (1997) 169–173.
[24] H.P. Choo, K.Y. Liew, W.A.K. Mahmood, H. Liu, J. Mater. Chem. 11 (2001) 2908.
[25] P.J.F. Harris, J. Catal. 97 (1986) 527–542.
[26] A.I. Kirkland, D.A. Jefferson, D.G. Duff, P.P. Edwards, I. Gameson, B.F.G. Johnson, D.J. Smith, Proc. R. Soc. Lond. A 440 (1993) 589–609.
[27] A.C. Curtis, D.G. Duff, P.P. Edwards, D.A. Jefferson, B.F.G. Johnson, A.I. Kirkland, A.S. Wallace, Angew. Chem. Int. Ed. Engl. 27 (1988) 1530–1533.
[28] L.D. Marks, Ultramicroscopy 18 (1985) 445–452.
[29] J.G. Allpress, J.V. Sanders, Aust. J. Phys. 23 (1970) 23–36.
[30] R. de Wit, J. Phys. C Solid State Phys. 5 (1972) 529–534.
[31] R.L. Penn, J.F. Banfield, Science 281 (1998) 971–989.
[32] D.G. Duff, A.C. Curtis, P.P. Edward, D.A. Jefferson, B.F.G. Johnson, A.I. Kirkland, D.E. Logan, Angew. Chem. Int. Ed. Engl. 26 (1987) 676–678.
[33] H. Hofmeister, Cryst. Res. Technol. 33 (1998) 3–25.
[34] D.G. Duff, A.C. Curtis, P.P. Edwards, D.A. Jefferson, B.F.G. Johnson, D.E. Logan, J. Chem. Soc. Chem. Commun. (1987) 1264–1266.
[35] Q.F. Zhou, J. Bao, Z. Xu, J. Mater. Chem. 12 (2002) 384–387.
[36] D.G. Duff, P.P. Edwards, B.F.G. Johnson, J. Phys. Chem. 99 (43) (1995) 15934–15944.
[37] I. Pastoriza-Santos, L.M. Liz-Marzán, Pure Appl. Chem. 72 (1–2) (2000) 83–90.
[38] M. Petroski, Z.L. Wang, T.C. Green, M.A. El-Sayed, J. Phys. Chem. B 102 (18) (1998) 3316–3320.
[39] L.D. Marks, Ultramicroscopy 18 (1985) 445–452.
[40] D.G. Duff, P.P. Edwards, B.F.G. Johnson, J. Phys. Chem. 99 (43) (1995) 15934–15944.
[41] T. Teranishi, M. Hosoe, T. Tanaka, M. Miyake, Chem. Mater. 10 (2) (1999) 594–600.